In: A. Bracciali (ed.), Proceedings of the 8th International Conference on Contact Mechanics and Wear of Rail/Wheel Systems (CM2009), Firenze, Italy, September 15-18, 2009.

REFINEMENT OF KALKER'S ROLLING CONTACT MODEL

dr.ir. E.A.H. Vollebregt*

*DIAM - Delft Institute of Applied Mathematics,
Delft University of Technology

*e.a.h.vollebregt@tudelft.nl

ABSTRACT

Improvements to Kalker's rolling contact model are presented. Firstly these concern refinements that allow larger problem sizes to be solved. Secondly, a difficulty is identified in the discretisation of the slip at the leading edge of the contact zone. In the original method, opposing particles of the contacting bodies are brought into contact too early, instead of when they enter the contact zone. This falsely increases the tangential tractions and deformations and leads to slip at the leading edge of the contact zone. This further introduces unphysical irregularities in the solution when the time step is chosen too large. These unwanted effects are eliminated by refining the discretisation of the slip. Finally we describe experiments to increase the order of accuracy of the model. Our results indicate that bilinear instead of piecewise constant elements are not beneficial, but that an improved approximation of the position of the leading edge might be helpful instead.

1 INTRODUCTION

A difficult problem in mechanical engineering concerns the rolling contact problem. Two bodies are pressed together such that a contact area is formed. Then the bodies are moved in a rolling motion with respect to each other. Particles of the bodies' surfaces move through the contact zone, with a speed comparable to that of opposing particles of the other body's surface. Under the influence of frictional forces, the bodies may adhere to each other in part of the contact area and slip over each other in other parts. This results in technologically important phenonema such as creepage, deformation and wear [6, 8].

Rolling contact theories exist in different forms, ranging from analytic formulae [5, 15, 16], simplified models [7, 13] or table-lookup schemes [9], all for fast evaluation of the nonlinear spin-creep-force law, via boundary element approaches (BEM) [8, 11, 14, 21] that provide more detailed insight in the stress distribution in the contact zone and its subsurface, but are restricted to specific (simplified) geometries and materials configurations, to more generic but slower finite element models (FEM) [1, 4, 10, 12, 20, 22, 23].

In this we are concerned with the variational theory for rolling contact mechanics by Prof. J.J. Kalker. This theory is regarded as an exact theory for concentrated frictional contact problems. This highly regarded method was implemented by Kalker in the computer program CONTACT [8, 18]. In recent years we made several extensions to this program. These extensions allowed us to use larger problem sizes, but two new problems are also encountered:

1. The results show unphysical artefacts when a time step size is used that is too large compared to the grid size in rolling direction;
2. The aggregate results, such as the total contact force, converge only linearly when the grid is refined.

In this paper we present our solution to the first problem and discuss work in progress by which the latter should be solved.

2 THE 3D ROLLING CONTACT PROBLEM

The program CONTACT is meant for:

- 3D homogeneous elastic and visco-elastic materials, which may be different for the two contacting bodies,
- with concentrated contact, i.e. where the resulting geometries are essentially flat in and near the contact zone, but not necessarily Hertzian,
- with dry friction, solving shifts as well as rolling, transient as well as steady state problems, with creepages and/or total forces prescribed,
- solving for the surface tractions first, but capable of computing the interior field as well.

The program is based on an influence function method. The elasticity equations for the interiors of the two contacting bodies are converted to equations for their bounding surfaces.

$$u_i(x) = \int_C A_{ij}(x,y)\, p_j(y)\, ds \tag{1}$$

The influence functions for the 3D elastic half-space are used, which are known analytically due to Boussinesq and Cerutti, see e.g. [3, 6]. Two important quantities of the contact problem are:

normal problem :

$$\text{deformed distance} \qquad e := h + u_n \tag{2}$$

tangential problem :

$$\text{slip} \qquad s_\tau := \dot{x}_\tau + \dot{u}_\tau \tag{3}$$

With these quantities the contact problem is to determine the contact region C, its subdivision into adhesion and slip areas H and S, and the tractions p_n, p_τ such that the following contact conditions are satisfied:

normal problem :

$$\text{in exterior E :} \quad e > 0,\ p_n = 0 \tag{4}$$

$$\text{in contact C = H+S :} \quad e = 0,\ p_n \geq 0 \tag{5}$$

tangential problem :

$$\text{in exterior E :} \quad s_\tau \text{ free},\ p_\tau = 0, \tag{6}$$

$$\text{in adhesion H :} \quad |s_\tau| = 0,\ |p_\tau| \leq g, \tag{7}$$

$$\text{in slip S :} \quad |s_\tau| > 0,\ |p_\tau| = g \tag{8}$$

Kalker has shown that this problem may be converted into a variational form. When disregarding inertial effects (quasi-static approach), the solution of the contact problem maximizes the so-called "complementary energy" C of the system. This is important for investigation of the existance and uniqueness of the solution. Further the formulation as an optimisation problem allows to use solution techniques that are guaranteed to converge.

In CONTACT a calculation starts by defining a potential contact area that encompasses the true contact area. The potential contact area is discretised into rectangular elements of size $\delta x \cdot \delta y$. The surface tractions are approximated by piecewise constant functions per element. This leads to

$$u_i(x_I) = \sum_j \sum_J A_{IiJj}(x_I, x_J)\, p_j(x_J) \tag{9}$$

Here x_I and x_J stand for the coordinates of rectangular elements I and J. A_{IiJj} stands for the influence coefficients. These are obtained by integrating (1) over a single element J with respect to an observation point at x_I, which can be done analytically [8]. Due to the choice for rectangular elements, the influence coefficients A_{IiJj} are identical for all pairs I, J for which the relative positions are the same.

The slip s_τ at the surface of the contacting bodies involves a time-derivative. It is discretised using a "previous time instance" t', with $\delta t = t - t'$. A related quantity is the traversed distance per time step $\delta q = V \cdot \delta t$, with V the rolling speed. δq is also called the "time step" for brevity. The displacements at the previous time instance are denoted by u'.

The resulting optimisation problem is solved using Kalker's active set algorithms NORM, TANG and KOMBI, in which the proper element divisions are iteratively solved [8]. For the normal problem this yields a set of linear equations that is solved using the Conjugate Gradients method. The tangential problem with slip results in a set of non-linear equations that are solved using the ConvexGS solver, a specific Gauss-Seidel type approach that determines the element divisions along the way [17].

3 IMPROVEMENTS FOR SOLVING LARGER PROBLEMS

In 2005 we created a look-up table for the creep-force-moment law for use in the VAMPIRE analysis program [19]. During this work we studied the total forces computed by CONTACT in detail. An initial result used in the validation of the table is shown in Figure 1. This figure concerns a test-case that showed the largest differences between our new and some existing results. The test-case concerns pure longitudinal creepage for a wide elliptical contact region, with ratio of semi-axes $a/b = 0.2$ ($a = 5\,mm, F_n/G = 1.3$).

In the investigation of these results we focused on the situation with (scaled) creepage magnitude $V_p = 0.7$ (creepage $\xi = 0.00857$, friction coefficient $\mu = 0.3$, $F_x = 0.725\, F_n$). It appeared that the computed total forces depend critically on the discretisation parameter δq, see Figure 2. This figure shows the total force F_x as a function of the time step parameter δq for different discretisation grids. This raised questions on the appropriate setting of the input parameter δq.

Note: the parameter δq has been a nuisance for a very long time. Kalker used to solve steady state contact problems for different values of δq, e.g. $\delta q = 2.0/1.0/0.5 \cdot \delta x$, and extrapolate the results to $\delta q = 0$. This approach was abandoned in the early 1990's because it didn't work well and complicated the com-

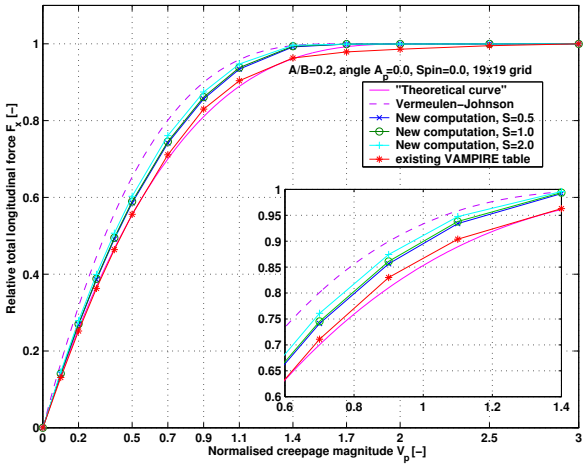

Figure 1: *Initial validation results (before model-improvement) for the new Vampire-table. Computed relative total longitudinal force F_x as a function of creepage magnitude V_p, compared to existing results.*

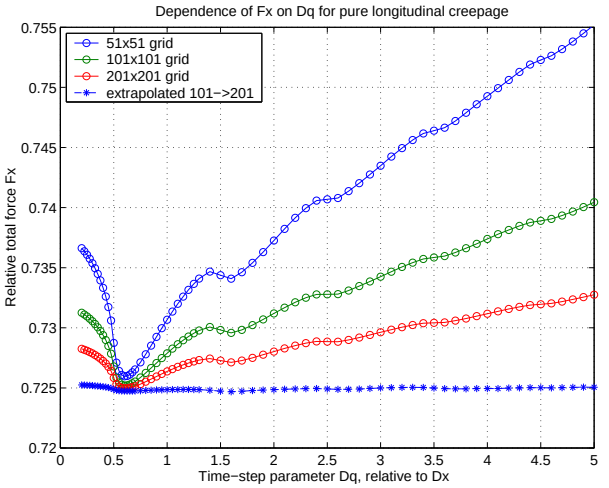

Figure 2: *Dependency of total force F_x on the discretisation grid and discretisation parameter δq for creepage magnitude $V_p = 0.7$.*

puter code. δq further has a strong influence on the convergence of the solution procedures. The ConvexGS solver did not work well when δq was chosen too small.

These convergence-problems of the ConvexGS solver appear to be remedied by using so-called relaxation in the solution process. The basic step in the solver is to solve the tractions $p^*_{I\tau}$ for one element I with the tractions in all other elements fixed. Relaxation means to enlarge or reduce the step with respect to the previous iterate $p^k_{I\tau}$ by a factor ω:

$$p^{k+1}_{I\tau} = p^k_{I\tau} + \omega \left(p^*_{I\tau} - p^k_{I\tau}\right) \tag{10}$$

For steady state problems and when using small time steps δq, under-relaxation ($\omega < 1$) improves the robustness and convergence speed. For instationary problems a bit of over-relaxation ($\omega > 1$) appears to be beneficial. It appears to be crucial to apply relaxation to the elements in the adhesion area, which is easy, as well as to the elements in the slip area, which is more difficult. Namely, direct application of (10) for an element in the slip area would lead to tractions that are not on the traction bound. This is solved by applying relaxation on the direction of the tractions:

$$\begin{aligned} &\text{solve for } p^*_{I\tau}, \text{ then set } p^{k+1}_{I\tau} \text{ such that} \\ &\arg p^{k+1}_{I\tau} = \arg p^k_{I\tau} + \omega \left(\arg p^*_{I\tau} - \arg p^k_{I\tau}\right) \end{aligned} \tag{11}$$

With this extended relaxtion procedure we get very good (robust) results.

The appropriate setting of δq was studied using very fine discretisation grids. In order to be able to use these grids several improvements were necessary:

- matrix-free implementations of the solvers were devised. These exploit the similarity of the influence coefficients for rectangular elements. The system matrix A for the tangential problem is dense and has size $2N \times 2N$, with N the number of elements in the contact zone. This means that for an 80×80 grid, with about 5.000 elements in the contact zone, about 0.8GB of internal memory is required. For a 100×100 grid this increases to about 2GB. However, all the elements on a diagonal of A are the same. By exploiting this similarity the memory requirements are reduced to 9 (pairs i, j) times $4N$, i.e. 3MB for a 100×100 grid.

- the main computational cores were parallelised using OpenMP, see e.g. [2]. This allows multi-processor/multi-core PC's to be used effectively. The corresponding speedup is shown in Table 1. This table shows the sequential and parallel execution times on an HP xw6600 workstation with two Intel Xeon E5420 quad core processors (2.5 GHz) and 8GB internal memory. For smaller problems the speedup is limited by computations that have not yet been parallelised, for large problems by exceeding the amount of cache memory. In between an excellent speedup is achieved.

With these extensions we have been able to solve larger problems and thus use finer discretisations than before. In the results presented thus far two additional observations may be made:

1. The results of the computations converge linearly

Problem size	seq. time	par. time	speedup
51×51	$12\,s$	$2.6\,s$	4.7
101×101	$263\,s$	$40\,s$	6.6
201×201	$6,806\,s$	$932\,s$	7.4
401×401	$163,806\,s$	$47,603\,s$	3.4

Table 1: *Speedup achieved for the steady state rolling test-case of section 3 by OpenMP parallelisation on an 8-core PC.*

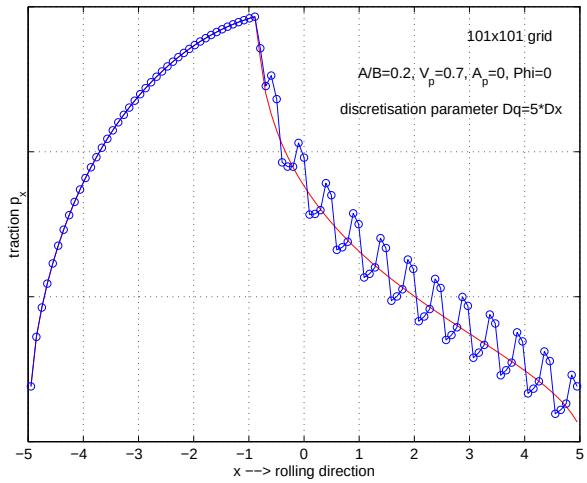

Figure 3: *An unphysical artefact in the results. Red line: correct results for time step $\delta q = \delta x$, blue: results for $\delta q = 5 \cdot \delta x$.*

when the grid sizes δx and δy are refined. This is illustrated in Figure 2, where the difference between the total forces of 51×51 and 101×101 grids are twice as large as between the forces computed for 101×101 and 201×201 grids. Note further that extrapolation to $\delta x = 0$ yields a result that is independent of δq as well.

2. The required computation time (for steady state problems) grows with $\mathcal{O}(N^{2.3})$. A factor N^2 stems from the full interaction between all elements ("dense system-matrix A"), the remaining $N^{0.3}$ from the increasing number of iterations in the solver ConvexGS.

As a consequence, doubling the accuracy requires about 25 times as much work. We come back to this issue in paragraph 5, but turn our attention to an unphysical artefact first.

4 BOUNDARY CONDITION AT THE LEADING EDGE

In this section we address an unphysical artefact that was discovered while studying the test-case "$V_p = 0.7$" that was described before. When the time step is chosen too large, the computed surface tractions display unphysical wavy irregularities. This is illustrated in Figure 3. The figure shows the tractions p_x at the centerline $y = 0$, computed on a 101×101 grid. The red line is the (correct) solution for time step $\delta q = \delta x$, the blue line is for $\delta q = 5\,\delta x$.

The artefacts appear for time steps δq larger than about $1.9\,\delta x$. The size of the irregularities grows slowly with growing δq. The period seems to be directly proportional to δq.

These irregularities appear to be caused by the discretisation of the shift (time-integrated slip) at the leading edge of the contact zone. This discretisation uses a particle fixed, Lagrangian approach. In this approach the shift is expressed as the sum of rigid shift plus deformation shift, where the deformation shift is the change in deformation of two contacting particles over a time step from t' to t.

$$S_{I\tau} = W_{I\tau} + u_{I\tau} - u'_{I\tau}. \tag{12}$$

Here $W_{I\tau}$ is the relative rigid shift of the bodies with respect to each other, i.e. the creepage integrated over a time step δt. $u_{I\tau}$ is the current deformation difference of two contacting particles at element I. And $u'_{I\tau}$ is the deformation of the same particles one time step earlier, at the position where they resided at time t'.

The problem with equation (12) is that it considers the opposing particles of the two bodies already to be in contact with each other at time t'. In a time step they are shifted with respect to each other over a distance of $W_{I\tau}$. Then traction must build up to annihilate this distance, to ensure that $S_{I\tau}$ becomes zero again. The first cell at the leading edge needs a lot of traction for this, and may even exceed the traction bound and slip. The second cell in the contact area needs less traction; since it was closer to the leading edge at time t' it had a larger previous displacement u'. This appears to lead to the wavy pattern that is illustrated in Figure 3.

In the continuous problem, the particles of bodies (1) and (2) are free to move with respect to each other as long as they haven't entered the contact zone. Consequently it is wrong to require annihilation of the full $W_{I\tau} = w_{I\tau} \cdot \delta t$. The build up of traction should be computed only for the fraction of the time step

that the particles reside in the contact zone, and for this the previous displacements u' must be adjusted as well. An appropriate discretisation of the shift appears to be the following.

$$S_{I\tau} = W_{I\tau} \cdot \frac{t - t_I^0}{\delta t} + u_{I\tau} - u_{I\tau}^0 \qquad (13)$$

Here t_I^0 is the moment in time when the center of element I enters the contact zone, and u_I^0 is the displacement difference between bodies (1) and (2) at that time.

In the computer implementation we assume that rolling takes place in the positive x-direction. For each row of the potential contact area we identify the highest cell number I in the contact zone S+H, with $I+1$ in the exterior region E. We assume that the true leading edge is located at

$$x_e = (1-\theta)x_I + \theta x_{I+1} \qquad (14)$$

with $\theta = 0.5$. Now the center of cell J that is located at x_J on time t, was located at $x_J + \delta q$ at time t'. This allows us to compute t_J^0:

$$t_J^0 = t - \frac{(x_e - x_J)}{\delta q}\delta t \qquad (15)$$

It then remains to approximate $u_{J\tau}^0$. This is done by extrapolating the displacements at previous time t' to x_e.

$$u_{J\tau}^0 = u'_{I+1,\tau} + \theta \cdot (u'_{I+1,\tau} - u'_{I+2,\tau}) \qquad (16)$$

Note that this approximation is independent of J.

This approach works well for instationary problems and for stationary problems that are solved using the DUVOROL approach, i.e. solving instationary problems until the steady state sets in. It is more difficult to combine with Kalker's direct approach for the steady state problem. This direct approach uses a matrix $A - A'$ instead of the original matrix A, with A' defined such that $u' = A'\,p$ (compare to equation (9)). For this an additional quantity is used in the iteration process for the adjustment of $u_{J\tau}^0$ conform equation (16).

Results obtained with this procedure are shown in Figures 4, 5 and 6. In Figure 4 the computed tractions along centerline $y = 0$ are shown for time steps $\delta q = 5\,\delta x$ (blue) and $\delta q = \delta x$ (magenta), and for $\delta q = \delta x$ for the original method (red). This graph shows that the artefact is gone. Further the results have become nearly independent of the time step δq. Finally, a substantial improvement is achieved over the original results for $\delta q = \delta x$. The new method

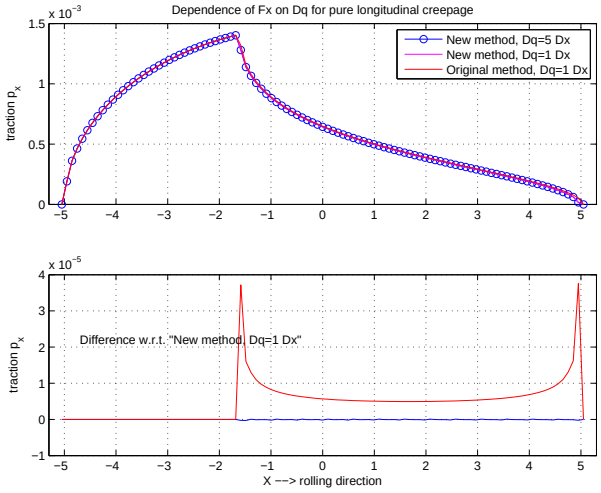

Figure 4: *Results obtained using the correction of (13) at the leading edge, compare to Figure 3.*

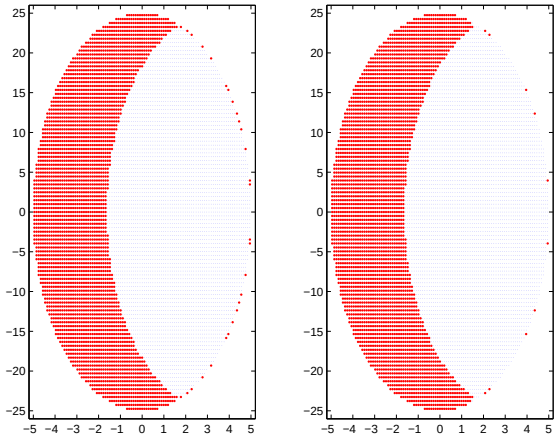

Figure 5: *Adhesion and slip areas for the original (left) and new methods (right). Note that the new method has less slip at the leading edge of the contact zone.*

leads to lower tangential tractions in the adhesion zone.

Figure 5 shows that the number of slipping elements near the leading edge of the contact area is reduced. The remaining slipping elements are attributed firstly to the approximation of an elliptical contact area by the union of rectangular elements, which yields rather small normal pressures in some of the elements at the edge of the contact area. Secondly, the choice of $\theta = 0.5$ is of influence. When θ is reduced, a smaller portion of $W_{I\tau}$ must be annihilated, see (13). However, this actually leads to a worse approximation of the total tangential force.

Figure 6 shows the aggregate results, i.e. the resulting

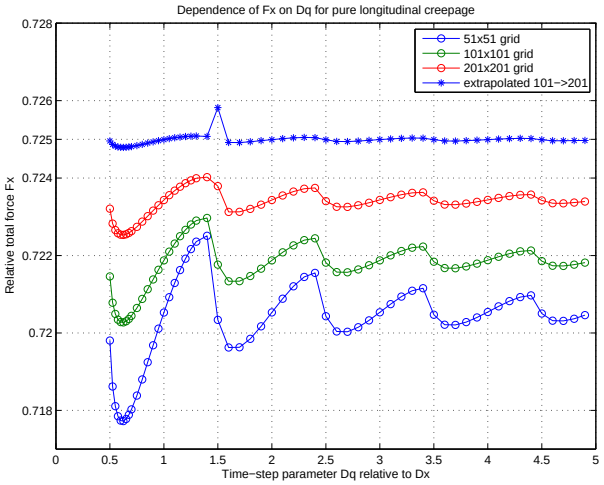

Figure 6: *Dependency of F_x on the discretisation grid and parameter δq, obtained using the correction of (13) at the leading edge, compare to Figure 2.*

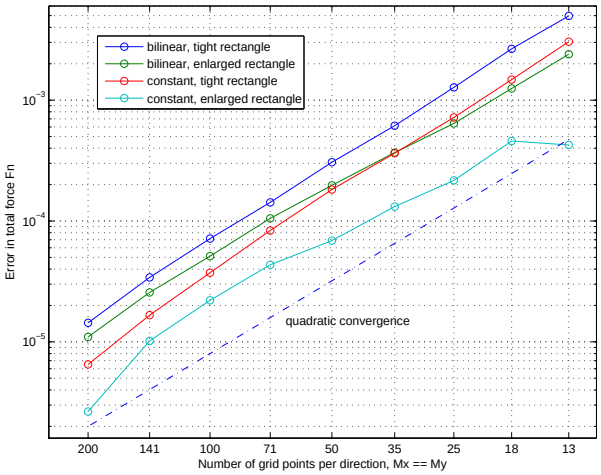

Figure 7: *Convergence of F_n when refining the discretisation grid, for piecewise constant and bilinear approximations of the tractions, and for potential contact areas that fit tightly around the true contact or that are enlarged and shifted by a half grid space.*

total force F_x. This graph shows that the results are much less dependent on the time step δq. The accuracy of the results is improved too, by roughly 30% at $\delta q = \delta x$. The order of convergence is however still the same.

5 IMPROVING THE ORDER OF ACCURACY

We now turn to the problem that was put forward at the end of paragraph 3, where it was found that doubling the accuracy requires 25 times as much work. This is problematic because the benefit of CONTACT with respect to approximate theories is its accuracy. It makes no sense to incorporate non-Hertzian effects in a simulation when these effects are small compared to the discretisation errors that are made. But when computation times are high, then it is prohibited to use CONTACT in an encompassing (vehicle dynamics, multi body) simulation program.

In order to improve the order of accuracy of CONTACT we tried switching from piece-wise constant to bilinear elements. For an element with size $\delta x \times \delta y$ that is centered around the origin, the following basis function is defined:

$$f^{elm}(x,y) = \begin{cases} (1-|x|/\delta x)\cdot(1-|y|/\delta y) & \text{for} \\ & |x|<\delta x \wedge |y|<\delta y \\ 0 & \text{otherwise} \end{cases} \tag{17}$$

For element J this basis function is shifted to the element center at (x_J, y_J). With this basis function the continuous tractions $p_j(x,y)$ are approximated by

$$p_j(x,y) = \sum_J p_{Jj} f_J^{elm}(x,y) \tag{18}$$

This approximation may be inserted in equation (1). The integrals may be evaluated per element, by which influence coefficients are defined analogously to equation (9). The corresponding integrals per element have been worked out analytically in [3]. These expressions are quite elaborate. In order to validate the ideas we first implemented an ad hoc approach. This consists of approximating the bilinear basis function (17) using a piece-wise constant function on, for instance, 50×50 sub-elements.

Our initial results with this approach are disappointing, and do not show any improvement over the original approach.

We first consider the normal problem, for which quadratic convergence is already achieved with the original approach. The total force computed for successively refined grids is illustrated in Figure 7.

Two different lines are presented both for the orignal and for the new approach. These lines illustrate a difficulty in the investigation of grid convergence. The computed tractions and resulting total force are strongly affected by the precise placement of the discretisation grid with respect to the true contact area. This is due to the slope discontinuity and the $\sqrt{h}$ behaviour of the tractions at the edge of the contact zone. It appears to be beneficial to dislocate the grid by a half grid space with respect to a potential con-

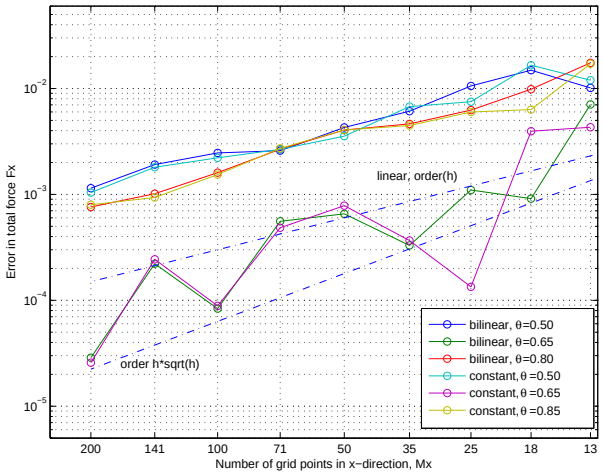

Figure 8: *Convergence of F_x when refining the discretisation grid, for piecewise constant and bilinear approximations of the tractions, with varying θ.*

tact area that is tightly fitted around the true contact area.

The quadratic convergence is understood by analogy to the numerical integration of $\sqrt{\max(0, 1 - x^2 - y^2)}$ over the unit square. Piecewise constant and bilinear approximations of the surface pressures may be compared to using midpoint and trapezoidal integration rules. With these rules, the same quadratic order of convergence is obtained. The convergence appears to be limited by the sampling errors at the edge of the contact zone. Note that this does not explain why the bilinear approximation performs significantly worse than the piecewise constant approach.

Our initial results for the tangential problem are shown in Figure 8. This figure shows that the parameter θ that was introduced in equation 14 has a strong influence on the results. For the most plausible value, $\theta = 0.5$, that approximates the edge of the contact zone with the edges of the rectangular elements, linear convergence of the total force is obtained. With a slightly higher value of $\theta = 0.65$, the error seems to behave like $\mathcal{O}(h\sqrt{h})$. Irrespective of θ, the results are comparable for piecewise constant and bilinear elements.

A notable difference between the normal and tangential problems is that local errors now have a more widespread effect. An error in the approximated position of the leading edge has an effect on the tractions for all neighbouring elements in the rolling direction in the adhesion zone. Therefore the position of the leading edge seems to be a key element for improving the accuracy of the approach.

6 CONCLUSIONS

In this paper we have discussed the rolling contact model developed by Prof. Kalker of Delft University of Technology. This model comprises the first and most comprehensive description of non-Hertzian three-dimensional bodies in rolling contact with dry friction. As such it forms the basis for different BEM and FEM simulation codes.

We concentrated on Kalker's implementation of the method in the CONTACT program. We described extensions of this program that further increased the speed and robustness of the solution approach. This allows larger computations and more detailed simulations to be performed.

An important difficulty in the discretisation of the slip or shift between the contacting bodies was identified. This difficulty ficticiously increases the surface tractions near the leading edge of the contact zone, which leads to higher tractions in the rest of the contact zone as well. It further leads to serious artefacts in the computational results when the time step is chosen too large. It appears to be caused by the treatment of the slip at the leading edge of the contact zone. An additional boundary condition must be imposed. We have shown that this modification eliminates the artefacts and improves the accuracy of the discretisation as well.

Finally our initial experiments with bilinear instead of piecewise constant approximations for the surface tractions have been shown. With these experiments we strive towards a lower computational complexity of the model, i.e. allowing for a more detailed resolution of the contact stresses using fewer elements. That would open the way to incorporate this contact model in vehicle dynamics simulation codes, for instance for the investigation of damage and wear. Our results indicate that bilinear elements do not improve the accuracy, but that one should try to improve the approximation of the position of the leading edge instead.

REFERENCES

[1] S. Bogdanski, M. Olzak, and J. Stupnicki. Numerical modeling of 3D rail RCF squat-type crack under operating load. *Wear*, 191:14–24, 1996.

[2] B. Chapman, G. Jost, and R. van der Pas. *Using OpenMP; Portable Shared Memory Parallel Programming.* MIT Press, 2008.

[3] J.R. Dydo and H.R. Busby. Elasticity solutions for constant and linearly varying loads applied to a rectangular surface patch on the elastic halfspace. *Journal of Elasticity*, 38:153–163, 1995.

[4] J.A. González, K.C. Park, C.A. Felippa, and R. Abascal. A formulation based on localized lagrange multipliers for BEM-FEM coupling in contact problems. *Computer Methods in Applied Mechanics and Engineering*, 197:623–640, 2008.

[5] K.L. Johnson. The effect of spin upon the rolling motion of an elastic sphere upon a plane. *Journal of Applied Mechanics*, 25:332–338, 1958.

[6] K.L. Johnson. *Contact Mechanics*. Cambridge University Press, Cambridge (UK), 1985.

[7] J.J. Kalker. A fast algorithm for the simplified theory of rolling contact. *Vehicle System Dynamics*, 11:1–13, 1982.

[8] J.J. Kalker. *Three-Dimensional Elastic Bodies in Rolling Contact*. Solid Mechanics and its Applications. Kluwer Academic Publishers, 1990.

[9] J.J. Kalker. Book of tables for the Hertzian creep-force law. In I. Zobory, editor, *Proceedings of the 2nd Mini Conference on Contact mechanics and Wear of Wheel/Rail systems*, pages 11–20, Budapest, Hungary, 1996.

[10] T.A. Laursen and I. Stanciulescu. An algorithm for incorporation of frictional sliding conditions within a steady state rolling framework. *Commun. in Numer. Meth. in Engng*, 22:301–318, 2006.

[11] Zili Li. *Wheel-rail rolling contact and its application to wear simulation*. PhD thesis, Delft University of Technology, 2002.

[12] U. Nackenhorst. The ALE-formulation of bodies in rolling contact - Theoretical foundations and finite element approach. *Comp. Meth. Appl. Mech. Eng.*, 193:4299–4322, 2004.

[13] J. Piotrowski and W. Kik. A simplified model of wheel/rail contact mechanics for non-Hertzian problems and its application in rail vehicle dynamics simulations. *Vehicle System Dynamics*, 46(1-2):27–48, 2008.

[14] I.A. Polonsky and L.M. Keer. A numerical method for solving rough contact problems based on the multi-level multi-summation and conjugate gradients techniques. *Wear*, 231:206–219, 1999.

[15] Z.Y. Shen, J.K. Hedrick, and J.A. Elkins. A comparison of alternative creep-force models for rail vehicle dynamic analysis. In J.K. Hedrick, editor, *The Dynamics of Vehicles. Proceedings of the 8th IA VSD Symposium*, Cambridge, MA, 1984. MIT.

[16] P.J. Vermeulen and K.L. Johnson. Contact of nonspherical bodies transmitting tangential forces. *Journal of Applied Mechanics*, 31:338–340, 1964.

[17] E.A.H. Vollebregt. A Gauss-Seidel type solver for special convex programs, with application to frictional contact mechanics. *Journal of Optimization Theory and Applications*, 87(1):47–67, 1995.

[18] E.A.H. Vollebregt. Contact'93 users manual. Technical Report TR00-07, VORtech, Postbus 260, 2600 AG Delft, august 2000.

[19] E.A.H. Vollebregt. On the calculation of a new Kalker-table for VAMPIRE. Memo EV/M05.031, version 1.0, VORtech, July 2005.

[20] M. Wiest, E. Kassa, W. Daves, J.C.O. Nielsen, and H. Ossberger. Assessment of methods for calculating contact pressure in wheel-rail/switch contact. *Wear*, 265:1439–1445, 2008.

[21] K. Willner. Fully coupled frictional contact using elastic halfspace theory. *ASME Journal of Tribology*, 130:031405–1/8, 2008.

[22] P. Wriggers. *Computational Contact Mechanics, 2nd ed.* Springer, Heidelberg, 2006.

[23] X. Zhao, Z. Li, C. Esveld, and R. Dollevoet. The effects of the tangential traction on wheel-rail dynamic contact. *WSEAS Trans. on Appl. and Theor. Mechanics*, 2:52–59, 2007.